Composite fermionization of 1-D Bose-Bose mixtures

Sascha Zöllner,[1,*] Hans-Dieter Meyer,[1] and Peter Schmelcher[1,2,†]

[1]*Theoretische Chemie, Universität Heidelberg, INF 229, 69120 Heidelberg, Germany*
[2]*Physikalisches Institut, Universität Heidelberg, Philosophenweg 12, 69120 Heidelberg, Germany*

(Dated: May 6, 2008)

We study the ground states of one-dimensional Bose-Bose mixtures under harmonic confinement. As we vary the inter-species coupling strength up to the limit of infinite repulsion, we observe a generalized, *composite-fermionization* crossover. The initially coexisting phases demix as a whole (for weak intra-species interactions) and separate on an atomic level (for strong intra-species repulsion). By symmetry, the two components end up with strongly overlapping profiles, albeit sensitive to symmetry-breaking perturbations. Different pathways emerge in case the two components have different atom numbers, different intra-species interactions, or different masses and/or trap frequencies.

PACS numbers: 67.85.-d, 67.60.Bc, 03.75.Mn

I. INTRODUCTION

The availability of cold atoms has made it possible to realize many fundamental quantum systems. Building on the seminal realization of Bose-Einstein condensation [1, 2], mixtures composed of, say, two different atomic species have come into the research focus. Aside from Bose-Fermi [3, 4] or Fermi-Fermi mixtures [5], whose potential for studying phenomena as diverse as impurity effects or superconductivity has been recognized more recently, two-component bosonic mixtures have received much experimental [6, 7, 8, 9, 10] and theoretical attention (see [11, 12, 13, 14, 15, 16, 17, 18] and Refs. therein). The interplay between intra- and inter-species forces gives rise to many effects not accessible with single-component Bose gases, including phase separation and modified superfluid-insulator transitions [14, 15], quantum emulsions [16], and spin-charge separation [18].

Most studies so far have focused on the regime of relatively weak interactions, where the physics can be described well in terms of mean-field or—in lattice geometries—simple lowest-band models. However, interatomic forces can be experimentally tuned to a large extent via Feshbach resonances [19]. In particular, in quasi-one-dimensional systems, which emerge under strong transversal confinement, it is possible to exploit confinement-induced resonances [20] to explore the regime of strong correlations [21, 22]. For infinitely repulsive bosons, this is known as the fermionization limit, in allusion to the fact that the system can be mapped exactly to an ideal Fermi gas [23]. Here the exclusion principle in a sense emulates the effect of *hard-core* interactions, to the extent that the bosons share local aspects with their fermionic counterparts, whereas nonlocal properties such as their coherence and momentum distribution are very different. The basic crossover from the weakly interacting trapped Bose gas to the fermionization limit had been predicted from a thermodynamic-limit perspective [24, 25] and interpreted in terms of a mean-field picture [26]. By contrast, it is only recently that its *microscopic* mechanism has been investigated within an ab-initio framework [27, 28, 29, 30].

In this work, we tackle the obvious question of how the fermionization crossover for the one-component Bose gas extends to a trapped *two-component* mixture. By way of analogy, tuning the *inter-component* coupling strength to the infinitely repulsive regime (for fixed intra-species interactions) may be regarded as *composite fermionization*. Here, a recent study has extended the standard fermionization map to mixtures of two *identical* particle species with both intra- and inter-species *hard-core* interactions [31]. Apart from this special borderline case, little is known except for a classification of the low-energy modes in the harmonic-fluid approximation [11]. Here we study the crossover from weak to strongly repulsive couplings between two components under harmonic confinement. We will show that this composite fermionization can lead to demixing, and lay out how it depends on the intra-species interactions, on the densities of the two components, as well as on the masses and trapping parameters of each species.

Our paper is organized as follows. Section II introduces the model and briefly reviews the fermionization map and its extension to mixtures. In Sec. III, we give a concise presentation of the computational method. Section IV first explores the completely symmetric setup, where both components have equal atom numbers, interaction constants, masses, and see the same harmonic trap. The subsequent Sec. IV in turn shows what different phase-separation scenarios emerge if these constraints are relaxed one by one.

II. THEORETICAL BACKGROUND

A. Model

We consider a mixture of two distinguishable bosonic species, which we shall label "A" and "B". These may correspond to atoms with unequal nucleon numbers—be it different isotopes or altogether different species—or possibly different hyperfine states of one and the same species. Furthermore, we assume these to be confined to quasi-one dimension (1D),

*Electronic address: sascha.zoellner@pci.uni-heidelberg.de
†Electronic address: peter.schmelcher@pci.uni-heidelberg.de

such that the transverse degrees of freedom may be integrated out. The effective low-energy Hamiltonian for an arbitrary mixture of $N = N_{\rm A} + N_{\rm B}$ atoms then reads

$$H = \sum_{\sigma={\rm A,B}} H_\sigma + H_{\rm AB},$$

where the single-species Hamiltonian H_σ and the inter-species coupling $H_{\rm AB}$ read

$$\begin{aligned} H_\sigma &= \sum_{i=1}^{N_\sigma} \left[\frac{p_{\sigma,i}^2}{2M_\sigma} + U_\sigma(x_{\sigma,i}) \right] + \sum_{i<j} g_\sigma \delta(x_{\sigma,i} - x_{\sigma,j}) \\ H_{\rm AB} &= \sum_{a=1}^{N_{\rm A}} \sum_{b=1}^{N_{\rm B}} g_{\rm AB} \delta(x_{{\rm A},a} - x_{{\rm B},b}). \end{aligned}$$

Here we consider harmonic trapping potentials $U_\sigma(x) = \frac{1}{2} M_\sigma \omega_\sigma^2 x^2$. By rescaling to harmonic-oscillator units $a_{\rm A} \equiv \sqrt{\hbar/M_{\rm A}\omega_{\rm A}}$, one can eliminate $M_{\rm A} = \omega_{\rm A} = 1$ by exploiting the scaling

$$H_{\rm A}(M_{\rm A}, \omega_{\rm A}, g_{\rm A}; X_{\rm A}) = \hbar\omega_{\rm A} H_{\rm A}(1, 1, g'_{\rm A}; X'_{\rm A}),$$

with $X'_{\rm A} \equiv (x'_{{\rm A},1}, \ldots, x'_{{\rm A},N_{\rm A}}) \equiv X_{\rm A}/a_{\rm A}$ and $g'_{\rm A} \equiv g_{\rm A}\sqrt{M_{\rm A}/\hbar^3\omega_{\rm A}}$.

For numerical reasons, we regularize the delta-function interaction by a normalized Gaussian of width much smaller than the inter-particle distance; see Ref. [28] for details.

B. Fermionization

The (single-component) 1D Bose gas has the peculiar property that it is isomorphic to a system of identical fermions. In particular, the *standard* Bose-Fermi map relates the many-body wave function of hard-core bosons (obeying the boundary condition $\Psi|_{x_i=x_j} = 0, i < j$, which corresponds to taking the 1D interaction strength $g \to \infty$) to that of non-interacting fermions Ψ_-:

$$\Psi = A\Psi_-, \qquad A(X) := \prod_{i<j} \mathrm{sgn}(x_i - x_j).$$

Specifically, the ground state is given simply by the absolute value of the non-interacting fermionic ground state, $\Psi_0 = |\Psi_{-,0}|$. This makes it tempting to think of Pauli's exclusion principle as emulating the effect of the repulsive interactions (or vice versa), which is why the limit $g \to \infty$ is commonly referred to as *fermionization*. Note that, since $A^2 = 1$, all local quantities will coincide with that computed from the fermion state. Specifically, this is the case for the density $\rho_N = |\Psi|^2$ and any derived quantities, such as the reduced (one- or two-body) densities. However, nonlocal quantities such as the momentum distribution, may differ dramatically from the fermionic ones.

The standard Bose-Fermi map above has recently been extended to mixtures of two *identical* species A = B (i.e., equal masses and potentials) with hard-core *intra-* and *inter-species* interactions, $g_\sigma = g_{\rm AB} \to \infty$. Its wave function Ψ is transformed to that of a system of $N = \sum_\sigma N_\sigma$ identical fermions [31]. For the special case of A and B being bosonic, this *generalized* Bose-Fermi map $\Psi = A\Psi_-$ reads

$$A(X_{\rm A}, X_{\rm B}) = A_{\rm A}(X_{\rm A}) A_{\rm B}(X_{\rm B}) A_{\rm AB}(X_{\rm A}, X_{\rm B}), \quad (1)$$

where $A_\sigma(X_\sigma) \equiv \prod_{1\le i<j\le N_\sigma} \mathrm{sgn}(x_{\sigma,i} - x_{\sigma,j})$ is the standard map restricted to subsystem σ, and $A_{\rm AB}(X_{\rm A}, X_{\rm B}) \equiv \prod_{a=1}^{N_{\rm A}} \prod_{b=1}^{N_{\rm B}} \mathrm{sgn}(x_{{\rm A},a} - x_{{\rm B},b})$ serves to impose hard-core boundary conditions on inter-species collision points. In the case of harmonic trapping, where the single-particle orbitals are known analytically, the solution may even be written down explicitly [31]

$$\Psi\left(X \equiv (X_{\rm A}, X_{\rm B})\right) \propto e^{-|X|^2/2} \prod_{1\le i<j\le N} |x_i - x_j|. \quad (2)$$

III. COMPUTATIONAL METHOD

Our approach relies on the numerically exact Multi-Configuration Time-Dependent Hartree method [32, 33], a quantum-dynamics tool which has been applied successfully to systems of few identical bosons (see [28, 29, 34, 35, 36]). Its principal idea is to solve the time-dependent Schrödinger equation $i\dot\Psi(t) = H\Psi(t)$ as an initial-value problem by expanding the solution in terms of direct (or Hartree) products $\Phi_J \equiv \varphi_{j_1}^{(1)} \otimes \cdots \otimes \varphi_{j_N}^{(N)}$:

$$\Psi(t) = \sum_J A_J(t) \Phi_J(t). \quad (3)$$

The (unknown) *single-particle functions* $\varphi_j^{(\kappa)}$ ($j = 1, \ldots, n_\kappa$) are in turn represented in a fixed *primitive* basis implemented on a grid. In our case of, where particles of each species are indistinguishable, the single-particle functions within each subset $\kappa \in \{1, \ldots, N_{\rm A}\}$ and $\{N_{\rm A}+1, \ldots, N\}$ are of course identical (i.e., we have $\{\varphi_{j_\sigma}^{(\sigma)}\}$, with $j_\sigma \le n_\sigma$). This, along with the correct symmetrization of the expansion coefficients A_J, ensures permutation symmetry within each subset A,B.

Note that in the above expansion not only the coefficients A_J but also the single particle functions φ_j are time dependent. Using the Dirac-Frenkel variational principle, one can derive equations of motion for both A_J, φ_j [33]. Integrating this differential-equation system allows us to obtain the time evolution of the system via (3). This has the advantage that the basis $\{\Phi_J(t)\}$ is variationally optimal at each time t. Thus it can be kept relatively small, rendering the procedure very efficient.

Although designed for time-dependent simulations, it is also possible to apply this approach to stationary states. This is done via the so-called *relaxation method* [37]. The key idea is to propagate some wave function $\Psi(0)$ by the non-unitary $e^{-H\tau}$ (*propagation in imaginary time*.) As $\tau \to \infty$, this exponentially damps out any contribution but that stemming from the true ground state like $e^{-(E_m - E_0)\tau}$. In practice, one relies on a more sophisticated scheme termed *improved relaxation*

[38], which is much more robust especially for excitations. Here $\langle\Psi|H|\Psi\rangle$ is minimized with respect to both the coefficients A_J and the orbitals φ_j. The effective eigenvalue problems thus obtained are then solved iteratively by first solving for A_J with *fixed* orbitals and then 'optimizing' φ_j by propagating them in imaginary time over a short period. That cycle will then be repeated.

IV. COMPOSITE-FERMIONIZATION TRANSITION

In contrast to the case of a single bosonic species, binary mixtures offer a plethora of different parameters, making the physics richer and less straightforward: In principle, we may have different atom numbers $N = N_{\rm A} + N_{\rm B}$, different masses $M_{\sigma={\rm A,B}}$, intra- and inter-species couplings g_σ ($g_{\rm AB}$), and species-dependent traps $U_\sigma(x)$. In this section, in order to illustrate the basic mechanism of the crossover from weak to strongly repulsive inter-species interactions, $g_{\rm AB} \in [0,\infty)$, we focus on the simplest, symmetric setup where

$$N_\sigma = \frac{N}{2};\ M_\sigma = 1;\ g_\sigma = g;\ U_\sigma(x) = \frac{1}{2}x^2 \quad (\sigma = {\rm A,B}).$$

In this case, H has an exact permutation symmetry between species A and B. This idealized situation may correspond to two internal states of the same species or, ignoring slight mass deviations, two different isotopes, where $g_{\rm AB}$ is tuned via the inter-species scattering length. Actually, in the special case where $g_\sigma = g_{\rm AB} = g$, this system maps to a one-component Bose gas with $N = \sum_\sigma N_\sigma$ atoms [28, 29, 30] (for any number of components and any N_σ, for that matter) – up to permutational degeneracies, which are not that severe for the ground state.

Here, by contrast, we are interest in the following question: What happens to the mixture— g_σ being fixed—when $g_{\rm AB}$ is varied up to the hard-core limit? (This we refer to as *composite fermionization* of the subsystems A and B, despite the general lack of a Bose-Fermi mapping as Eq. 1.) To get an impression of that crossover, let us start with the case of two almost ideal Bose gases, $g_\sigma = 0.4$, each consisting of $N_\sigma = 2$ atoms (similar results hold for larger atom numbers). Figure 1 displays the evolution of the density profile $\rho(x) \equiv \rho_\sigma(x)$, measuring the probability distribution for finding one σ atom at position x. Obviously, for $g_{\rm AB} \to 0$, the total state $\Psi = \Psi_{\rm A} \otimes \Psi_{\rm B}$ simply consists of two uncorrelated "condensates" ($\Psi_\sigma = \phi_0^{\otimes N_\sigma}$ for $g = 0$), slightly smeared out due to repulsion. Increasing $g_{\rm AB}$ leads to an ever deeper dip in the profiles. This should be contrasted with the case of two *single* fermionized bosons, $N_\sigma = 1$ [39]. The dip in Fig. 1 is much more pronounced, which is indicative of phase separation, if symmetry screened: $\rho_{\rm A} = \rho_{\rm B}$ are completely identical by symmetry. However, this only corresponds to an ensemble average – in a *single* measurement, we will always find all $N_{\rm A}$ atoms on one side of the trap and $N_{\rm B}$ atoms on the other. This claim is underscored by Fig. 1(*bottom*), which reveals the evolution of the two-body densities $\rho_{\sigma,\sigma'}$. If we were to measure, say, the first A-type boson at $x_{{\rm A},1} \approx 1$, then we are sure to find the second A boson also in that region $x_{{\rm A},2} \approx 1$

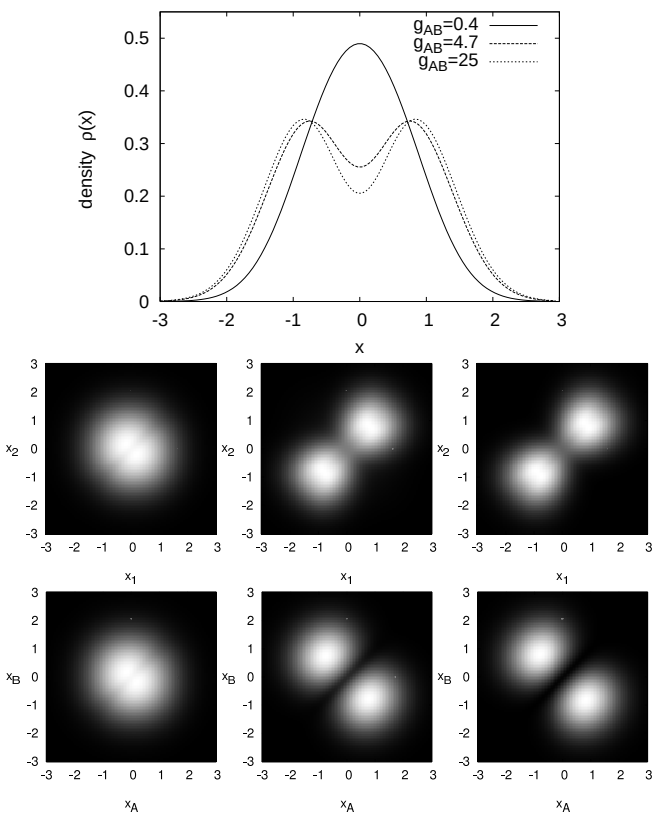

Figure 1: Composite fermionization of a mixture with $N_{\sigma={\rm A,B}} = 2$ bosons with intra-component interaction $g_\sigma = 0.4$. *Top*: density profiles $\rho(x)$; *Bottom*: Two-body correlation functions $\rho_{\sigma\sigma}(x_1, x_2)$ and $\rho_{\rm AB}(x_{\rm A}, x_{\rm B})$ for inter-species couplings $g_{\rm AB} = 0.4,\ 4.7$ and 25 (from left to right).

and not on the left, and *vice versa*. By contrast, the probability for subsequently finding a B particle at the same position is virtually zero, as dictated by the hard-core boundary condition, $\Psi|_{x_{{\rm A},a}=x_{{\rm B},b}} = 0$ ($g_{\rm AB} \to \infty$). This makes it tempting to think of this an entangled state of the form

$$|N_{\rm A}, 0\rangle \otimes |0, N_{\rm B}\rangle + |0, N_{\rm A}\rangle \otimes |N_{\rm B}, 0\rangle,$$

where $|n_{\rm L}, n_{\rm R}\rangle \in \mathbb{H}_\sigma$ denotes a state with $n_{\rm L,R}$ atoms localized on the left (right). It should be noted that, even for $g_\sigma = 0$, there is no simple mapping to fermions as (1), since the hard-core condition is imposed only on inter-species collision points, and thus the information about which fragment the individual coordinates belong to needs to be retained. However, in our special case of a harmonic trap, it is natural to conjecture that the exact solution is given by a modification of the single-species fermionization limit [40],

$$\Psi_{g_{\rm AB}\to\infty}(X) \propto e^{-|X|^2/2} \prod_{a\le N_{\rm A}, b\le N_{\rm B}} |x_{{\rm A},a} - x_{{\rm B},b}|,$$

which obeys the correct boundary conditions at points of inter-species collisions. Trusting that logic, an analogous extension should hold for the homogeneous system [23].

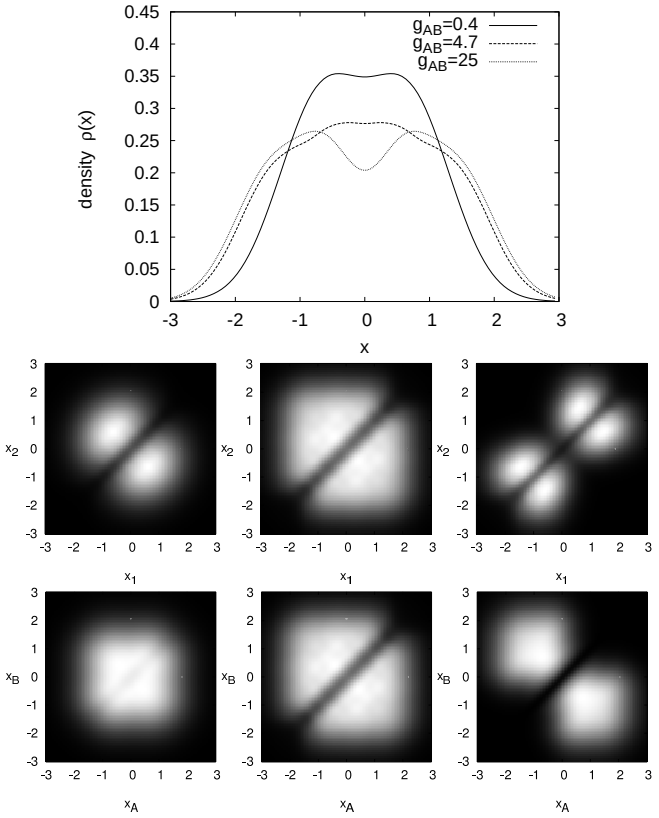

Figure 2: Same as Fig. 1, but with $g_{\rm A} = g_{\rm B} = 4.7$.

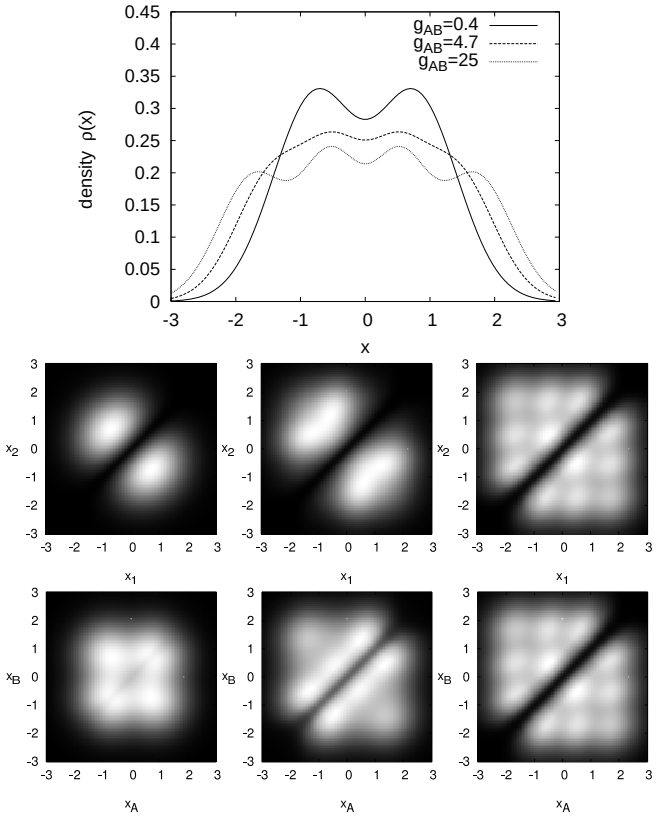

Figure 3: Same as Fig. 1, but with $g_{\rm A} = g_{\rm B} = 25$.

A similar pathway is encountered for two more strongly interacting components, $g_\sigma = 4.7$ (see Fig. 2, *top*). At $g_{\rm AB} = 0.4$, we have more or less two uncorrelated clouds, which are governed by the desire to reduce their *intra*-species interaction energy. As $g_{\rm AB} = 4.7$ reaches g_σ, this turns into a trade-off between avoiding the own species just as much as the other component. Letting $g_{\rm AB} \to \infty$, the inter-particle repulsion takes over, and a similar phase-separation tendency of A and B as before may be recognized in Fig. 2. In contrast to the "condensate" case, however, the separation of the two peaks is not pronounced as each hump is quite smeared out in itself due to the intra-species repulsion. This is illuminated further by the two-body densities (Fig. 2): Here the pattern for $\rho_{\sigma\sigma}(x_1, x_2)$ at $g_{\rm AB} = 25$ is modulated by a correlation hole at $x_1 = x_2$ due to intra-species repulsion, as compared to the weakly interacting components (Fig. 1). This explains the two broadened peaks in $\rho_\sigma(x)$.

So far, we have seen that the components tend to separate when the inter-species repulsion overwhelms the intra-species one. This naturally brings up the question of the fate of two initially fermionized components, as shown for $g_\sigma = 25$ in Fig. 3. Notably, by the conventional Bose-Fermi map, this relates to a Fermi-Fermi mixture. Weak couplings $g_{\rm AB} = 0.4$ pass the two fermionized clouds largely unnoticed, which exhibit $N_\sigma = 2$ characteristic humps in $\rho_\sigma(x)$ [40]. However, for larger values $g_{\rm AB} = 4.7$, the profiles slowly rearrange to a more complex structure, which culminates in a profile with $N = 4$ wiggles at $g_{\rm AB} = g_\sigma = 25$. The density oscillations signify that *each* of the four atoms seeks an isolated spot, irrespective of its species. That interpretation is supported by the plots of the two-body densities $\rho_{\sigma\sigma} = \rho_{\rm AB}$, which for $g_{\rm AB} = 25$ reveal the checkerboard pattern familiar from the single-boson crossover [28]. This should be contrasted with the intermediate regime where $g_{\rm AB} = 4.7 < g_\sigma$: Here two, say, A atoms are still localized on the left and on the right side as for $g_{\rm AB} = 0$. Upon measuring an A atom at, say, $x_{\rm A} \approx 1.5$, the two B atoms will likely be found at either $x_{\rm B} \approx 0.5$ or $x_{\rm B} \approx -1.5$, this way remaining isolated from each other but also avoiding the A atom.

Note that, in agreement with our earlier remarks, the case $g_\sigma = g_{\rm AB}$ relates to a single-component Bose gas, which in turn maps to an ideal *Fermi* gas via (1) in the limit $g_{\rm AB} \to \infty$. As in that case, for $N \gg 1$ these N peaks become ever tinier modulations on the envelope density, which for a harmonic trap can be computed as $\bar\rho(x) = \sqrt{2N - x^2}/N\pi$ [41].

At this stage, we should point out that this limit is highly degenerate: For one thing, there is a permutation degeneracy between A and B particles. Second, in the limit $g_{\rm AB} \to \infty$, the ground-state wave function (which is non-negative) degenerates with the fermionic one by the Bose-Fermi map and, since no specific permutation symmetry is imposed when treating the two components as distinguishable, all solutions even with mixed A-B-exchange statistics are permissible [31].

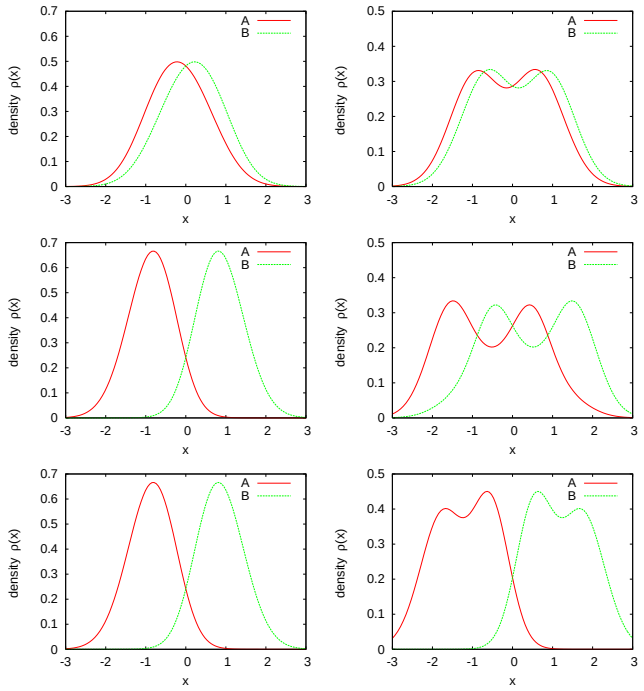

Figure 4: (color online) Instability under symmetry-breaking perturbation, $U_\sigma(x) = \frac{1}{2}x^2 + d_\sigma x$ ($d_\mathrm{A} = -d_\mathrm{B} = 0.1$). *Left*: Densities $\rho_\sigma(x)$ for $g_\sigma = 0.4$; *Right*: $g_\sigma = 25$. Shown are the coupling strengths $g_\mathrm{AB} = 0.4, 4.7, 25$ from top to bottom.

Symmetry-breaking instability. By permutation symmetry of H between A and B, the density profiles ρ_σ are identical, even in the limit $g_\mathrm{AB} \gg g_\sigma$, and thus trivially cannot exhibit phase separation. However, if we deal with two different species, it is conceivable that these two feel slightly different trapping potentials, where the deviations are much weaker than the mean trapping and inter-particle forces but only serve to break the symmetry. In particular, imagine that $U_\sigma(x) = \frac{1}{2}x^2 + d_\sigma x$, such that the trap centers be shifted by $d_\mathrm{A} = -d_\mathrm{B} \ll 1$, see Fig. 4. Expectedly, for weak couplings g_AB, the profiles are barely affected. However, toward stronger inter-species repulsion, this tiny perturbation is the last straw needed to make the two phases demix completely. Similar results hold also for different densities, $N_\mathrm{A} \neq N_\mathrm{B}$. This makes it even more inviting to think of the symmetric profiles in Figs. 1–3 as averages over the equivalent configurations with A (B) being on the left (right), and the other way around.

V. PHASE-SEPARATION SCENARIOS

So far, we have studied a completely symmetric setup, where only the inter-species interactions were permitted to differ. This way, a symmetry-breaking perturbation was needed to reveal the hidden phase separation. Although not experimentally unrealistic, this scenario is somewhat artificial. We now want to relax the above symmetry constraints step by step and discuss the wealth of different demixing pathways if the two components have different particle numbers (Sec. V A), different internal interaction strengths (Sec. V B), and have different masses and/or trap frequencies (Sec. V C).

A. Density-assisted demixing

An obvious question regarding our findings in the previous section is: What happens in the case of unequal particle numbers, $N_\mathrm{A} \neq N_\mathrm{B}$? Figure 5 illustrates this on the example of two weakly interacting components, $g_\sigma = 0.4$ (*left column*), where $N_\mathrm{A} = 3$ is larger than $N_\mathrm{B} = 2$. As the Bose-Bose coupling gets stronger, $g_\mathrm{AB} = 1.3$, one observes that the low-density phase B moves to the outer edge, thus "sandwiching" high-density A component in the middle. This well-known phenomenon traces back to the fact that the coupling energy $\langle H_\mathrm{AB}\rangle = N_\mathrm{A}N_\mathrm{B}g_\mathrm{AB}\int \rho_\mathrm{AB}(x,x)dx$ scales with $N_\mathrm{A}N_\mathrm{B}$ compared to the individual energies $\langle H_\sigma\rangle \propto N_\sigma$. Thus for the smaller B component, it is less expensive to move to the higher potential regions. Not unexpectedly, we have found this to be even more pronounced for $N_\mathrm{A} \gg N_\mathrm{B}$. Note that, close to the composite-fermionization limit ($g_\mathrm{AB} = 4.7,\ 25$), both components develop two humps in the density, if much more pronounced for B. This is indicative of a superposition state similar to that in Sec. IV: The B atoms are found on the right and the A atoms on the left, and *vice versa*, only that the shift for A is much smaller due to their higher density.

A similar pathway again exists for non-negligible intra-component interactions, $g_\sigma = 4.7$ (Fig. 5). As $g_\mathrm{AB} \to \infty$, the initially mixed phases separate: The profile $\rho_\mathrm{A}(x)$ develops a clear-cut peak at $x = 0$, whereas B is again driven to the boundary. Even though, on the face of it, this looks different from the weakly interacting case, this density pattern can be understood in complete analogy: The two components are isolated on the left and on the right, respectively; however, due to the larger atom number N_A and the repulsion pressure, A tends to be more in the center *on average*.

An entirely different situation is encountered in the "Fermi-Fermi"-like setup with $g_\sigma = 25$ (Fig. 5). For intermediate $g_\mathrm{AB} = 15 < g_\sigma$, a phase forms where the A atoms localize at three discrete spots such that the two B atoms fill the two holes in between. For $g_\mathrm{AB} = 25$, by contrast, the N atoms completely localize atom by atom just like in the case of a 2+2 mixture, in agreement with the extended Bose-Fermi map (1). In analogy to Sec. IV, these will demix under slight symmetry-breaking perturbations into one phase with $N_\mathrm{A} = 3$ density wiggles on, say, the left side, and $N_\mathrm{B} = 2$ on the right.

B. Interaction-assisted demixing

Up until now, we have assumed comparable interactions within each component. Of course, it is of fundamental concern what the composite-fermionization crossover looks like in the case where one species is more strongly repulsive, including as a special case a "Bose-Fermi"-type mixture of one weakly interacting and another, fermionized component.

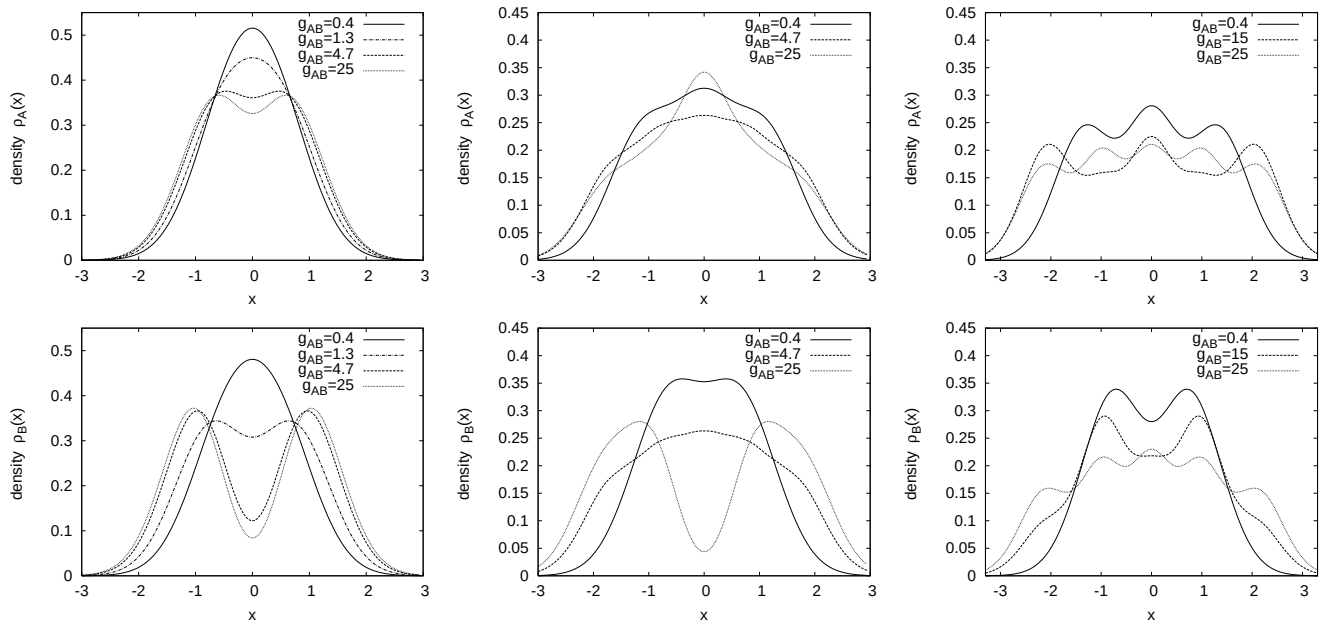

Figure 5: Demixing for different particle numbers $N_{\rm A} = 3$, $N_{\rm B} = 2$: Density profiles $\rho_{\rm A}(x)$ (top) and $\rho_{\rm B}(x)$ (bottom) for intra-species interaction strengths $g_\sigma = 0.4,\ 4.7$ and 25 (from left to right).

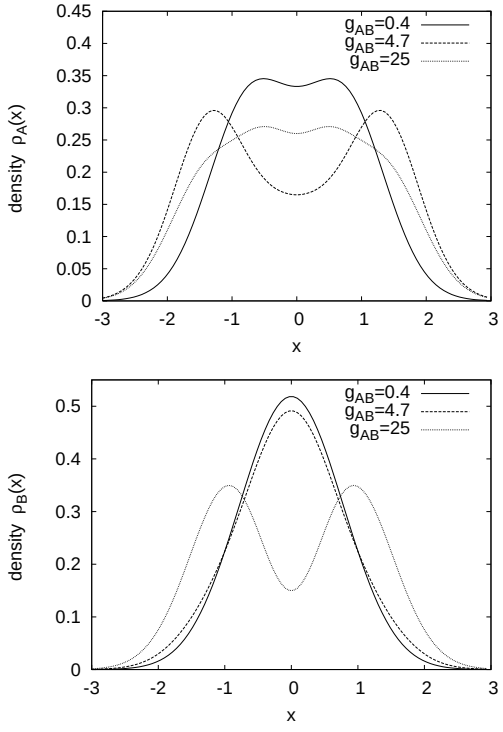

Figure 6: Demixing for different intra-component interactions $g_{\rm A} = 4.7$, $g_{\rm B} = 0.4$: Density profiles $\rho_{\rm A}(x)$ (top) and $\rho_{\rm B}(x)$ (bottom) for an $N_\sigma = 2$ mixture at different couplings $g_{\rm AB} = 0.4,\ 4.7$ and 25.

An illustrative example is given in Fig. 6, displaying the composite-fermionization crossover for an $N_\sigma = 2$ mixture with $g_{\rm A} = 4.7 > g_{\rm B} = 0.4$. We distinguish two regimes:

1. For $g_{\rm AB} < g_{\rm A}$, the weakly interacting central B cloud is barely affected; at the same time, the strongly interacting A bosons move slightly to the outside, thus cutting down on both intra- and inter-species interaction energy.

2. By contrast, for $g_{\rm AB} = 25 > g_{\rm A}$, this partial separation is no longer enough: Now the B cloud splits up, signifying the formation of the entangled state discussed before with $N_{\rm A}$ atoms on the left and $N_{\rm B}$ atoms on the right, and *vice versa*. Note that, owing to the strong inter-species repulsion in A, the two humps in $\rho_{\rm A}$ are washed out strongly.

We stress that only regime (1.) exists for a Bose-Fermi-type mixture, i.e., where $g_{\rm A} \to \infty$: The minimum-energy state for infinitely large $g_{\rm AB}$ then has all B atoms in the center and A on the edges.

Coherence aspects. At this point, it is worthwhile dwelling for a moment on the coherence properties of bosonic mixtures, as reflected in the reduced one-body density matrix $\rho_\sigma(x,x') \equiv \langle x|\hat{\rho}_\sigma^{(1)}|x'\rangle$ and, closely related, the momentum distribution

$$\tilde{\rho}_\sigma(k) \equiv 2\pi\langle k|\hat{\rho}_\sigma^{(1)}|k\rangle = \int dx \int dx' e^{-ik(x-x')}\rho_\sigma(x,x').$$

It has been demonstrated for *identical* bosons [29, 30] how, in the course of fermionization, the zero-momentum peak $\tilde{\rho}(k=0)$—related to the fraction of condensed bosons—is attenuated and redistributed toward higher momenta, culminating in a characteristic decay $\tilde{\rho}(k) \overset{k\to\infty}{\sim} ck^{-4}$ as predicted for hard-core short-range interactions [42]. Equivalently, the off-diagonal long-range order, measured by $\rho_1(x,-x)$ as $x \to \infty$,

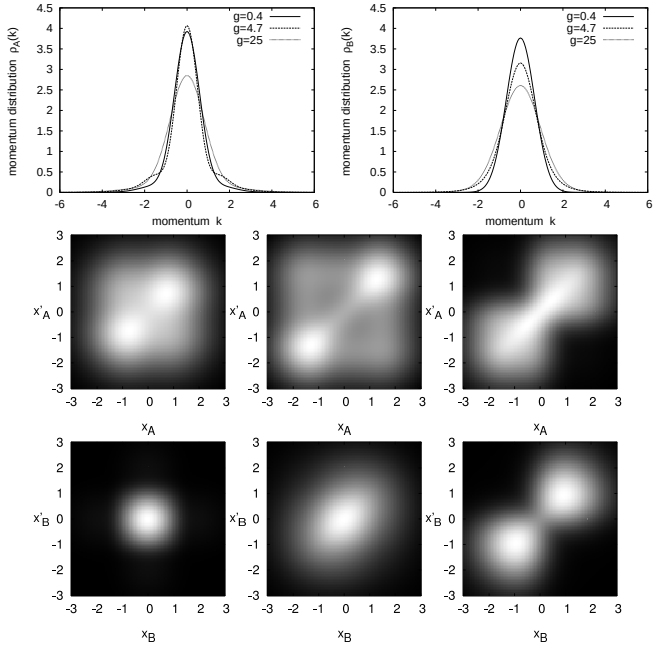

Figure 7: Coherence properties of the system in Fig. 6. *Top*: momentum distributions $\tilde{\rho}_\sigma(k)$; *Bottom*: One-body density matrices $\rho_\sigma(x_\sigma, x'_\sigma)$ for $g_{\rm AB} = 0.4,\ 4.7$ and 25 (from left to right).

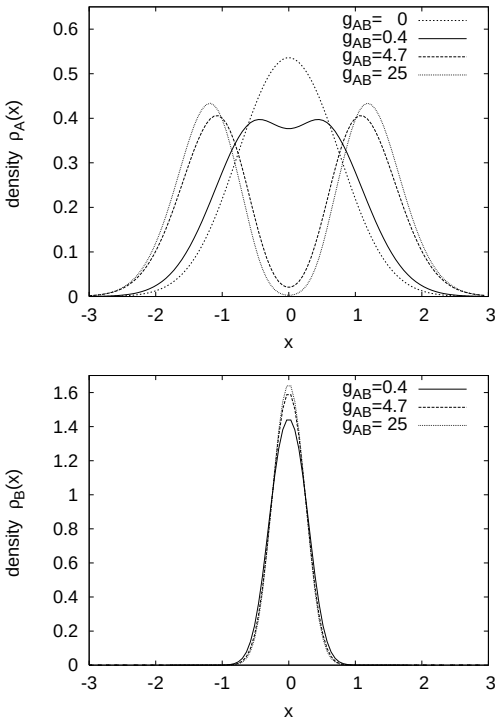

Figure 8: Demixing for different masses, $M_{\rm B}/M_{\rm A} = 9$: Density profiles $\rho_{\rm A}(x)$ (top) and $\rho_{\rm B}(x)$ (bottom) for a $2 + 2$ mixture with $g_\sigma = 0.4$ at different couplings $g_{\rm AB}$.

is strongly reduced. We generally find the same two mechanisms at work here, which we exemplify in Fig. 7. For stronger inter-species repulsion, the high-momentum tail in $\tilde{\rho}_\sigma(k)$ becomes more pronounced. Interestingly, for the component B with weaker interaction, the $k = 0$ peak starts diminishing right away, while the strongly repulsive A component first sees a sharpening at zero momentum ($g_{\rm AB} = 4.7$). This derives from its initial delocalization so as to move away from B [cf. $\rho_{\rm A}(x_{\rm A}, x'_{\rm A})$ in Fig. 7], which allows the A atoms to spend less kinetic energy $\langle \frac{1}{2}p^2 \rangle \propto (\Delta k)^2$.

C. Trap-induced demixing

After having explored the effect of different densities or interaction strengths on the composite-fermionization pathway, let us now relax the condition of equal masses and trapping potentials (*here*: frequencies). In this case, the system no longer maps to a single-component Bose gas even for $g_\sigma = g_{\rm AB}$.

1. Different confinement lengths

Assume that we have a nontrivial mass ratio, i.e., $M_{\rm B} > 1$ without loss of generality, with an otherwise symmetric parameter set. The effective oscillator length of the B atoms will then be reduced by a factor of $a_{\rm B} = 1/\sqrt{M_{\rm B}} < 1$. This situation is visualized in Fig. 8 for the choice $M_{\rm B} = 9$. At weak couplings, $\rho_{\rm B}(x)$ is simply constricted at the trap center, while $\rho_{\rm A}(x)$ extends over a much larger region. As we switch on the interaction between the components, the B atoms remain unmoved, whereas the A bosons are gradually driven toward the outside. This is intuitive: The former component roughly feels an average Hamiltonian

$$\bar{H}_{\rm B} = H_{\rm B} + {\rm tr}_{\rm A}[H_{\rm AB}\hat{\rho}_{\rm A}^{(N_{\rm A})}] = H_{\rm B} + g_{\rm AB}N_{\rm A}\sum_{b=1}^{N_{\rm B}}\rho_{\rm A}(x_{{\rm B},b}),$$

and likewise for A. Since the heavy B atoms are effectively frozen at the center, where $\rho_{\rm A}(x_{\rm B}) \approx \rho_{\rm A}(0)$ changes slowly, they only feel a constant energy shift due to the presence of A atoms. By contrast, the latter ones see an effective "potential barrier" $\rho_{\rm B}(x_{\rm A}) \approx \delta(x_{\rm A})$ which varies only in a small region about zero.

That phase-separation mechanism is largely insensitive to the intra-species interactions g_σ: We have confirmed these results also for, e.g., two quasi-fermionized components. Also note that a similar scale separation persist for the case of different frequencies but equal masses, i.e., $\omega_{\rm B}/\omega_{\rm A} \gg 1$. The different effective interaction felt by B, $g'_{\rm B} = g_{\rm B}\sqrt{M_{\rm B}/\omega_{\rm B}}$, and the modified energy scale, $\omega_{\rm B}$, do not qualitatively alter the picture above.

2. Different energy scales

Let us now look into the complementary case where the oscillator lengths be equal, $a_{\rm B} = 1/\sqrt{M_{\rm B}\omega_{\rm B}} = 1$, but such that

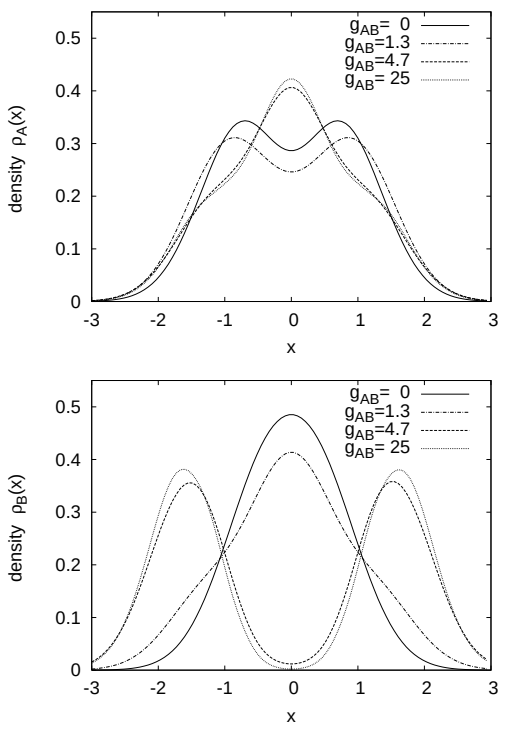

Figure 9: Demixing for different energy scales, $M_{\rm B} = 1/\omega_{\rm B} = 3$: Density profiles $\rho_{\rm A}(x)$ (top) and $\rho_{\rm B}(x)$ (bottom) for a $2+2$ mixture with $g_{\rm A} = 25$ and $g_{\rm B} = 0.4$, at different couplings $g_{\rm AB}$.

the energy scale $\omega_{\rm B} \neq 1$ shall be different. In order words, a stronger localization by virtue of a larger mass is compensated by a shallower trap for the B species. This option is sounded out in Fig. 9, where $M_{\rm B} = 3 = \omega_{\rm B}^{-1}$. The two profiles still overlap for weak couplings $g_{\rm AB} = 0, 1.3$. For sufficiently strong inter-species repulsion, though, it apparently becomes beneficial for the B atoms to spread out to larger x so as to segregate from A, which in turn is compressed on the inside. This is particularly striking in the setup captured in Fig. 9: Here the A component is squeezed even though it is fermionized and thus possesses a high internal pressure. The reason for that counter-intuitive behavior is simply that the potential-energy costs for the B phase are lower by $\omega_{\rm B} = 1/3$.

VI. CONCLUSION

We have studied binary few-boson mixtures in a one-dimensional harmonic trap throughout the crossover from weak coupling to strong inter-component repulsion. Depending on the intra-species interactions, different pathways to a new kind of "composite fermionization" have shown up: For two weakly interacting Bose gases, the two phases segregate as a whole, where the demixing for equal densities is obscured by symmetry-induced entanglement fragile to displacement of the trap. By contrast, for two strongly repulsive components, demixing occurs on the atomic level.

If one component has a lower density, then it tends to delocalize toward the outer edge, while the high-density phase is compressed in the center. Furthermore, in case one component is far more repulsive, the crossover exhibits an intermediate regime where that species forms a shell around the central, weakly interacting, component; only for large inter-species couplings do they fully segregate. This is accompanied by an increase (decrease) of the central momentum peak for the strongly (weakly) interacting species. Finally, for different mass or frequency ratios, one component freezes at the trap center, such that it acts as an effective potential barrier for the more mobile species.

The small mixtures of strongly repulsive atoms studied here should be experimentally accessible. The preparation and detection techniques required are similar to those already available for few bosons of a single species. The interaction forces may be tuned independently over a wide range by varying the (inter- and intra-species) scattering lengths as well as the transverse confinement, which parametrically modifies the effective one-dimensional coupling strengths.

Acknowledgments

Financial support from the Landesstiftung Baden-Württemberg in the framework of the project 'Mesoscopics and atom optics of small ensembles of ultracold atoms' is acknowledged by P.S. and S.Z.

[1] C. J. Pethick and H. Smith, *Bose-Einstein condensation in dilute gases* (Cambridge University Press, Cambridge, 2001).
[2] L. Pitaevskii and S. Stringari, *Bose-Einstein Condensation* (Oxford University Press, Oxford, 2003).
[3] A. G. Truscott *et al.*, Science **291**, 2570 (2001).
[4] Z. Hadzibabic *et al.*, Phys. Rev. Lett. **88**, 160401 (2002).
[5] M. Taglieber *et al.*, Phys. Rev. Lett. **100**, 010401 (2008).
[6] C. J. Myatt *et al.*, Phys. Rev. Lett. **78**, 586 (1997).
[7] D. S. Hall *et al.*, Phys. Rev. Lett. **81**, 1539 (1998).
[8] P. Maddaloni *et al.*, Phys. Rev. Lett. **85**, 2413 (2000).
[9] G. Modugno *et al.*, Phys. Rev. Lett. **89**, 190404 (2002).
[10] J. Catani *et al.*, Phys. Rev. A **77**, 011603 (2008).
[11] M. A. Cazalilla and A. F. Ho, Phys. Rev. Lett. **91**, 150403 (2003).
[12] Y.-Q. Li, S.-J. Gu, Z.-J. Ying, and U. Eckern, Europhys. Lett. **61**, 368 (2003).
[13] V. S. Shchesnovich, A. M. Kamchatnov, and R. A. Kraenkel, Phys. Rev. A **69**, 033601 (2004).
[14] O. E. Alon, A. I. Streltsov, and L. S. Cederbaum, Phys. Rev. Lett. **97**, 230403 (2006).
[15] T. Mishra, R. V. Pai, and B. P. Das, Phys. Rev. A **76**, 013604 (2007).
[16] T. Roscilde and J. I. Cirac, Phys. Rev. Lett. **98**, 190402 (2007).
[17] K. Nho and D. P. Landau, Phys. Rev. A **76**, 053610 (2007).
[18] A. Kleine *et al.*, Phys. Rev. A **77**, 013607 (2008).
[19] T. Köhler, K. Góral, and P. S. Julienne, Rev. Mod. Phys. **78**,

1311 (2006).
[20] M. Olshanii, Phys. Rev. Lett. **81**, 938 (1998).
[21] T. Kinoshita, T. Wenger, and D. S. Weiss, Science **305**, 1125 (2004).
[22] B. Paredes *et al.*, Nature **429**, 277 (2004).
[23] M. Girardeau, J. Math. Phys. **1**, 516 (1960).
[24] D. S. Petrov, G. V. Shlyapnikov, and J. T. M. Walraven, Phys. Rev. Lett. **85**, 3745 (2000).
[25] V. Dunjko, V. Lorent, and M. Olshanii, Phys. Rev. Lett. **86**, 5413 (2001).
[26] O. E. Alon and L. S. Cederbaum, Phys. Rev. Lett. **95**, 140402 (2005).
[27] Y. Hao, Y. Zhang, J. Q. Liang, and S. Chen, Phys. Rev. A **73**, 063617 (2006).
[28] S. Zöllner, H.-D. Meyer, and P. Schmelcher, Phys. Rev. A **74**, 053612 (2006).
[29] S. Zöllner, H.-D. Meyer, and P. Schmelcher, Phys. Rev. A **74**, 063611 (2006).
[30] F. Deuretzbacher, K. Bongs, K. Sengstock, and D. Pfannkuche, Phys. Rev. A **75**, 013614 (2007).
[31] M. D. Girardeau and A. Minguzzi, Phys. Rev. Lett. **99**, 230402 (2007).
[32] H.-D. Meyer, U. Manthe, and L. S. Cederbaum, Chem. Phys. Lett. **165**, 73 (1990).
[33] M. H. Beck, A. Jäckle, G. A. Worth, and H.-D. Meyer, Phys. Rep. **324**, 1 (2000).
[34] S. Zöllner, H.-D. Meyer, and P. Schmelcher, Phys. Rev. A **75**, 043608 (2007).
[35] S. Zöllner, H.-D. Meyer, and P. Schmelcher, Phys. Rev. Lett. **100**, 040401 (2008).
[36] S. Zöllner, H.-D. Meyer, and P. Schmelcher, arXiv:0801.1090v1 .
[37] R. Kosloff and H. Tal-Ezer, Chem. Phys. Lett. **127**, 223 (1986).
[38] H.-D. Meyer and G. A. Worth, Theor. Chem. Acc. **109**, 251 (2003).
[39] M. A. Cirone, K. Góral, K. Rzazewski, and M. Wilkens, J. Phys. B **34**, 4571 (2001).
[40] M. D. Girardeau, E. M. Wright, and J. M. Triscari, Phys. Rev. A **63**, 033601 (2001).
[41] E. B. Kolomeisky, T. J. Newman, J. P. Straley, and X. Qi, Phys. Rev. Lett. **85**, 1146 (2000).
[42] A. Minguzzi, P. Vignolo, and M. P. Tosi, Phys. Lett. A **294**, 222 (2002).